

# The histone deacetylase RPD3 counteracts genomic silencing in *Drosophila* and yeast

Francesco De Rubertis\*, David Kadosh†, Sandra Henchoz\*, Daniel Pauli\*, Gunter Reuter‡, Kevin Struhl† & Pierre Spierer\*

\* Department of Zoology and Animal Biology, University of Geneva, 30 quai E.-Ansermet, CH-1211 Geneva 4, Switzerland

† Department of Biological Chemistry and Molecular Pharmacology, Harvard Medical School, Boston, Massachusetts 02115, USA

‡ Institut für Genetik, Martin-Luther-Universität, D-06108 Halle/S, Germany

Both position-effect variegation (PEV)<sup>1,2</sup> in *Drosophila* and telomeric position-effect in yeast (TPE)<sup>3–5</sup> result from the mosaic inactivation of genes relocated next to a block of centromeric heterochromatin or next to telomeres. In many aspects, these phenomena are analogous to other epigenetic silencing mechanisms, such as the control of homeotic gene clusters<sup>6</sup>, X-chromosome inactivation<sup>7</sup> and imprinting in mammals<sup>8</sup>, and mating-type control in yeast<sup>5</sup>. Dominant mutations that suppress or enhance PEV are thought to encode either chromatin proteins or factors that directly affect chromatin structure<sup>1</sup>. We have identified an insertional mutation in *Drosophila* that enhances PEV and reduces transcription of the gene in the eye–antenna imaginal disc. The gene corresponds to that encoding the transcriptional regulator RPD3 in yeast<sup>9,10</sup>, and to a human histone deacetylase<sup>11</sup>. In yeast, *RRD3*-deletion strains show enhanced TPE, suggesting a conserved role of the histone deacetylase RPD3 in counteracting genomic silencing. This function of RPD3, which is in contrast to the general correlation between histone acetylation and increased

transcription, might be due to a specialized chromatin structure at silenced loci.

In the *w<sup>m4</sup>* inversion of *Drosophila melanogaster*, the *white* gene is relocated next to a breakpoint within centromeric heterochromatin, and can thus be permanently inactivated in some cells by spreading of the adjacent condensed heterochromatin<sup>1,2</sup> (Fig. 1). The resulting mottled eye-colour phenotype (Fig. 1a) is sensitive to the dose of several unlinked loci, known as suppressors and enhancers of position-effect variegation. These modifiers respectively decrease and increase the frequency of clones in which the gene is inactive<sup>1</sup>. The eye of a fly carrying a homozygous viable P-transposon insertion at 64 BC, on the third chromosome, is shown in Fig. 1b; the insertion enhances the variegation of *white*, which seems to be inactive in almost all ommatidia. In 5–10% of the eyes, patches of ommatidia show the disorganization characteristic of the phenotype of the *roughest* mutation, a locus near *white*, but more distant from heterochromatin in the rearrangement. This suggests that the enhancement of variegation allows the silencing to spread past the *white* locus, and to inactivate the *roughest* locus in a fraction of the cells (Fig. 1c, d). The mutation is homozygous viable, and the strong phenotype seems similar in homozygotes and heterozygotes.

In order to link the enhancer phenotype and the P-element insertion, excisions of the transposon were induced and found fully to revert the enhancer phenotype. The locus was cloned by plasmid rescue, and a single transcript of 2.2 kilobase (kb) long was detected on northern blots of embryonic, larval and adult RNA in a 20-kb genomic interval surrounding the insertion point. The P-element is inserted 1.8 kb from the 5' end of the transcript, in the putative regulatory region (Fig. 2). We were unable to find convincing differences in the developmental transcription profile between wild-type and mutant total RNA. However, *in situ* detection of transcripts on whole-mount larval imaginal discs revealed a significant reduction of transcript level in eye–antenna discs of homozygous *rp3* mutant flies (Fig. 2), whereas other discs from the same animals showed no clear difference, and eye–antenna discs exhibited normal staining for an unrelated gene (*dE2F*; data not shown). This result indicates that enhanced PEV results from the loss of RPD3 function in the phenotypically relevant tissue.

Complementary DNA clones were isolated from libraries of embryonic RNA<sup>12</sup>, and a clone with an insert of 2,172 nucleotides (a length similar to that of the 2.2-kb transcript on northern blots) was sequenced. An open reading frame encoding 520 amino acids is preceded by a 5' untranslated leader 223 bases long, and followed by a 3' untranslated sequence 389 bases long. Database analysis reveals that the transcript encodes a new gene in *Drosophila* that strongly resembles the human histone deacetylase RPD3, which has also been cloned in yeast, worm and frog<sup>9–11</sup> (Fig. 3).

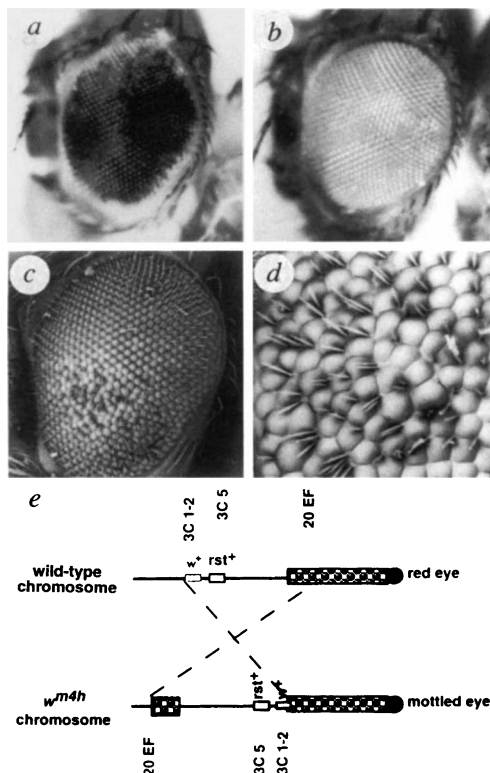


FIG. 1 Effect of an insertional mutation at 64 BC on PEV. a, b, Heads of males carrying the X-chromosome inversion *w<sup>m4h</sup>* (a), and carrying the same inversion together with the heterozygous mutation *Evar 15-1* (b). c, Scanning electron micrograph of the head of a fly of the same genotype as in b; d, enlargement of the *roughest* domain. e, Schematic representation of the *w<sup>m4h</sup>* inversion.

The high degree of similarity prompted us to test whether a mutation of yeast *RPD3* also affects position-effect variegation. In *Saccharomyces cerevisiae*, genes positioned up to 4.9 kb proximal to a telomere can be transcriptionally silenced, a phenomenon called telomeric position-effect (TPE)<sup>3-5</sup>. The closer a gene is located to the telomere, the greater is the silencing<sup>13</sup>. To measure TPE in yeast, we used isogenic wild-type *RPD3* and  $\Delta rpd3$  strains that contain a *URA3* gene positioned 2.0, 3.5 and 6.5 kb from the right end telomere of chromosome V<sup>13</sup>. *URA3* expression was monitored by growth on medium containing 5-fluoro-orotic acid (FOA), a drug that is toxic to cells expressing this gene. The  $\Delta rpd3$  strains containing the *URA3* gene positioned 2.0 and 3.5 kb from the telomere grew significantly better than did wild-type *RPD3* strains on FOA medium, demonstrating that an *rpd3* null allele increases telomeric silencing at these distances (Fig. 4).

Our results indicate that *RPD3* has an analogous function with respect to genomic silencing in both budding yeast and *Drosophila*. In both organisms, loss of *RPD3* function results in increased genomic silencing, which decreases with the distance from heterochromatin. Although we cannot exclude the possibility that *RPD3* indirectly affects genomic silencing (for example, by repressing the expression of a positive regulator of chromatin condensation), the striking similarity of *rpd3* mutant phenotypes in yeast and *Drosophila* strongly suggests that *RPD3* is directly involved in

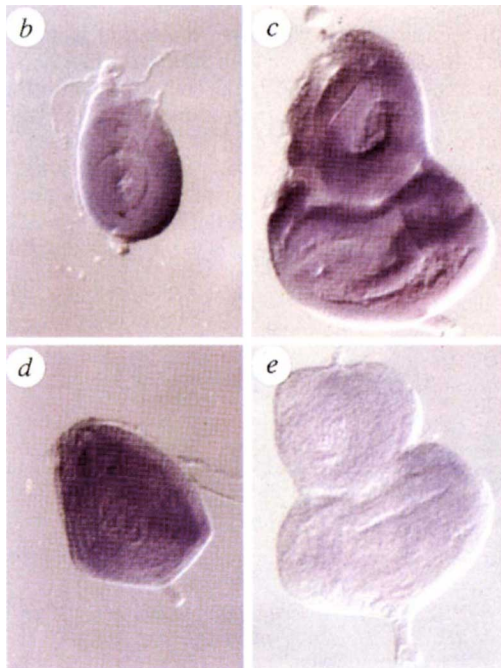
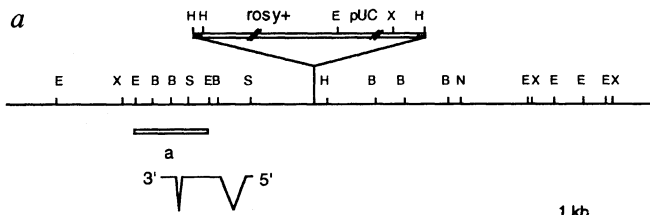


FIG. 2 Transcript accumulation in eye-antenna and leg imaginal discs of mutant and wild-type larvae. a, The 64B locus. The probe used for *in situ* hybridizations was fragment 'a'. b, Wild-type eye disc; c, wild-type eye antenna disc; d, mutant leg disc; e, mutant eye-antenna disc, in which expression of the gene is strongly reduced.

HD1	MAQTQGTTRKVCYIYDGDVGNVYYGQGHMPKPHRIRMTHN	
D-RPD3	MQSHSKRVCIYSDIIGNVYYGQGHMPKPHRIRMTHN	50
Y-RPD3	MVYEATPFDPITVKPSDKRRVAYFYDADVGNVYAGAGHPMKPHRIRMTHS	
HD1	LLLNYGLYRKMIEYRPHKANAEEMTKVHSDDYIKFLRSIRPDNMSEYSKQ	
D-RPD3	LLLNYGLYRKMIDI.RPHKATADEMTKFKHCEYVFLRSIRPDNMSEYNKQ	100
Y-RPD3	LIMNYGLYKMEIYRAKPAKQEMCQHFHDEYIDFLSRVTPDNLEMFKRE	
HD1	MQRFNVEDCVPFDGLFEFCQLSTGGSVASAVKLNKQOTDIAVNMAGGLH	
D-RPD3	MQRFNVEDCVPFDGLYEPFQLSAGGSVAAVKLNKQASEICTINWGGGLH	150
Y-RPD3	SVKFNVDGDCVPFDGLYEYCSISGGSMGGAARLNRGKCDVAVNVAGGLH	
HD1	HAKKSEASGFVNDIVLAILLELLKYHQRVLYIDIDIHGGDVVEAFYTT	
D-RPD3	HAKKSEASGFVNDIVLGIILELLKYHQRVLYIDIDVHHGGDVVEAFYTT	200
Y-RPD3	HAKKSEASGFVNDIVLGIILELLKYHQRVLYIDIDVHHGGDVVEAFYTT	
HD1	DRVMTVSFHKYGEYFPGTGLRDLIGAGKGYAVNPLRDGIDDESVEAI	
D-RPD3	DRVMTVSFHKYGEYFPGTGLRDLIGAGKGYAVNPLRDGMDDDAYESI	250
Y-RPD3	DRVMTCSFHKYGEYFPGTGELRDLIGAGKGYAVNPLRDGIDDATYRSV	
HD1	FKPVMKVMEMFQPSAVVLQCGSDLSGDRGCFNLTIKGHAKCVEFVKS	
D-RPD3	FVPIISKVMTFQPAAVVLQCGADSLTGDRGCFNLVKGHGKCVFVKK	300
Y-RPD3	FEPVIKIMEMYQPSAVVLQCGSDLSGDRGCFNLSMEGHANCVYKS	
HD1	FNLPLMLGGGGYTIKRVRCWTYETAVALDTEIPNELPYNDYFEYFGPD	
D-RPD3	YNLPLMLVGGGGYTIKRVRCWTYETAVALDTEIPNELPYNDYFEYFGPD	350
Y-RPD3	FGIPMMVGGGGYTMRNVARITWCFETGLLNVLKDLPLNYEYFEYFGPD	
HD1	FKLHISPSNMTNQNTNEYLEKIKQRLFENLRMLPHAPGVQMAIPEDAIP	
D-RPD3	FKLHISPSNMTNQNTSEYLEKIKNRLFENLRMLPHAPGVQIAIPEDAIP	400
Y-RPD3	YKLSVRPSNMFVNTPEYLDKVMNIPANLENKYAPSVQLNHTPRDAED	
HD1	EESGDEDEDDPKRISICSS DKRIACEEESDSEEEGEGGRKNSNF	
D-RPD3	DESDDKVDKDDRLPQ S. DKDKRIVPENYSDESEDEGEGGRDNRSY	450
Y-RPD3	LGDVEEDSAEAKDTKGG SQYARDLHVEHNEFY	
HD1	KKAKRVKTEDEKEKDPPEEKKEVTEEEKTKEEKPEAKGVKKEEVKLA	
D-RPD3	KGQRKRPRLDKDTNSNKASSETSSSEIKDEKEKGDGAGEESTASNTNSNN	500
D-RPD3	NSNNKSDNDAGATANAGSGSGSGSAGAKGAKENNI	537

FIG. 3 Comparison of the D-RPD3 deduced protein sequence with the human (HD1) and yeast homologues (Y-RPD3). A vertical bar indicates identical amino acids, and two dots indicate conserved amino acids. In the overlapping region, similarity is 82% (75% identity) with the human homologue, and 71% (58% identity) with yeast. Sequence comparison was done with the BLAST program.

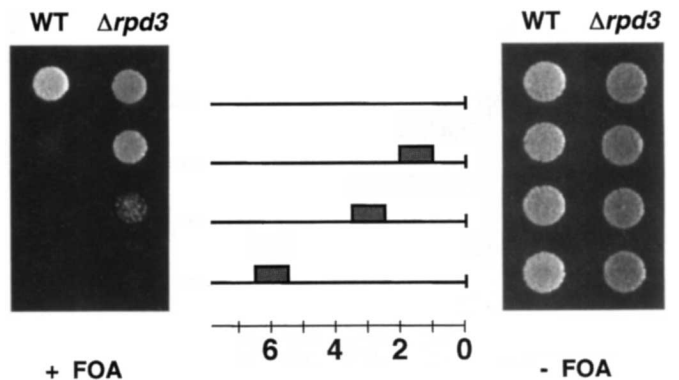


FIG. 4 Effect on yeast telomeric silencing. Parental strain YPH 250 lacks a functional *URA3* gene, whereas strains UCC506, UCC508 and UCC510 contain a *URA3* gene (shaded rectangle). In the three cases the gene is orientated such that transcription proceeds towards the telomere. Cells ( $10^3$ ) of wild-type (WT) and  $\Delta rpd3$  strains were spotted on plates in the presence (left) or the absence (right) of 5-FOA, and were incubated for 2 days at 30 °C.

counteracting genomic silencing.

Yeast and *Drosophila* RPD3 strongly resemble a human histone deacetylase<sup>11</sup>, and it is likely that the observed enhancement of genomic silencing is due to reduced activity of this enzyme. This conclusion is surprising because histone acetylation (which should be increased when RPD3 function is lost), is generally correlated with increased transcriptional activity<sup>14–20</sup>. However, there are precedents in yeast and *Drosophila* of such opposite actions, and of putative effects of acetylation on transcriptional repression. In yeast, *rp3* (*sds6*) mutations can restore the metastable repression in strains containing both a *rap1* mutant allele and a mutated silencer element<sup>21</sup>. Moreover, in the silenced mating-type loci, lysine 12 of histone H4 is acetylated, and this acetylation establishes transcriptional silencing<sup>22</sup>. In this regard, *rp3* mutant strains show increased acetylation of lysines 5 and 12 of histone H4 (ref. 23). In *Drosophila*, a particular isoform of histone H4 acetylated on lysine 12 is abundant in heterochromatin, whereas the other isoforms are underrepresented<sup>18</sup>. Lysines 5 and 12 of H4 are acetylated when newly synthesized histone is deposited, and are then rapidly deacetylated<sup>24</sup>. Here also RPD3, as a hypothetical deposition-related histone deacetylase, could support silencing<sup>22</sup>.

Thus a specific RPD3-dependent deacetylation could act as a negative signal in establishing a silencing protein complex. More generally, our results suggest that silenced loci may have specialized chromatin structures that are conserved between yeast and *Drosophila*. □

## Methods

**Whole-mount *in situ* hybridization.** This was done using digoxigenin-labelled probes<sup>25</sup>. The P-element used in the mutagenesis, and plasmid rescue have been described<sup>26</sup>.

**Yeast telomeric silencing.** Strains YPH250, UCC506, UCC508 and UCC510 were obtained from D. Gottschling, and have been described<sup>9</sup>. Strains were grown on glucose-minimal media containing casamino acids in the presence and absence of 5-fluoro-orotic acid (1 mg ml<sup>-1</sup>). To construct  $\Delta$ *rp3* strains, the *RPD3* coding region was obtained by genomic polymerase chain reaction (PCR) and cloned into pUC18. Sequences between the *Nsil* site and *Bam*HI site of *RPD3* were then replaced by the *Nsil*–*Bam*HI fragment containing the *HIS3* gene, and the resulting DNA was used to generate  $\Delta$ *rp3*::*HIS3* strains by one-step gene displacement.

Received 12 August; accepted 28 October 1996.

1. Reuter, G. & Spierer, P. *BioEssays* **14**, 605–612 (1992).
2. Karpen, G. H. *Curr. Opin. Genet. Dev.* **4**, 281–291 (1994).
3. Gottschling, D. E., Aparicio, O. M., Billington, B. L. & Zakian, V. A. *Cell* **63**, 751–762 (1990).
4. Aparicio, O. M., Billington, B. L. & Gottschling, D. E. *Cell* **66**, 1279–1287 (1991).
5. Laursen, P. & Rine, J. *Microbiol. Rev.* **56**, 543–560 (1992).
6. Paro, R. *Curr. Opin. Cell Biol.* **5**, 999–1005 (1993).
7. Gartler, S. M. & Riggs, A. D. *Annu. Rev. Genet.* **17**, 155–190 (1983).
8. Solter, D. *Annu. Rev. Genet.* **22**, 127–146 (1988).
9. Vidal, M. & Gaber, R. F. *Mol. Cell. Biol.* **11**, 6317–6327 (1991).
10. McKenzie, E. A. et al. *Mol. Gen. Genet.* **240**, 374–386 (1993).
11. Taunton, J., Hassig, C. A. & Schreiber, S. L. *Science* **272**, 408–411 (1996).
12. Brown, N. H. & Kafatos, F. C. *J. Mol. Biol.* **203**, 425–437 (1988).
13. Renaud, H. et al. *Genes Dev.* **7**, 1133–1145 (1993).
14. Turner, B. M. *J. Cell Sci.* **99**, 13–20 (1990).
15. Wolffe, A. P. & Pruss, D. *Cell* **84**, 817–819 (1996).
16. Brownell, J. E. & Allis, C. D. *Curr. Opin. Genet. Dev.* **6**, 176–184 (1996).
17. Braunstein, M., Rose, A. B., Holmes, S. G., Allis, C. D. & Broach, J. R. *Genes Dev.* **7**, 592–604 (1993).
18. Turner, B. M., Birley, A. J. & Lavender, J. *Cell* **69**, 375–384 (1992).
19. Jeppesen, P. & Turner, B. M. *Cell* **74**, 281–289 (1993).
20. Brownell, J. E. et al. *Cell* **84**, 843–851 (1996).
21. Sussell, L., Vannier, D. & Shore, D. *Genetics* **141**, 873–888 (1995).
22. Braunstein, M., Sobel, R. E., Allis, C. D., Turner, B. M. & Broach, J. R. *Mol. Cell. Biol.* **16**, 4349–4356 (1996).
23. Rundlett, S. E. et al. *Proc. Natl Acad. Sci. USA* **93**, 13723–13728 (1996).
24. Sobel, R. E., Cook, R. G., Perry, C. A., Annunziato, A. T. & Allis, C. D. *Proc. Natl Acad. Sci. USA* **92**, 1237–1241 (1995).
25. Masucci, J. D., Miltenberger, R. J. & Hoffmann, F. M. *Genes Dev.* **4**, 2011–2023 (1990).
26. Seum, C. et al. *Development* **122**, 1949–1956 (1996).

**ACKNOWLEDGEMENTS.** We thank A. Spierer for cytogenetic mapping of the locus; C.-H. Tonka for technical assistance; D. Gottschling for yeast strains; and M. Collart for suggesting this collaboration. This work was supported by grants from the Swiss National Science Foundation (P.S. and D.P.), the State of Geneva, and by grants from the National Institute of Health (U.S.) and the German Research Foundation (G.R.).

**CORRESPONDENCE** and requests for materials should be addressed to P.S. (e-mail: spierer@sc2a.unige.ch). The nucleotide sequence has been deposited in the EMBL Nucleotide Sequence Database, accession no. Y09258.

# Crystal structure of the GTPase-activating domain of human p120GAP and implications for the interaction with Ras

Klaus Scheffzek\*, Alfred Lautwein†‡, Wolfgang Kabsch†, Mohammad Reza Ahmadian\* & Alfred Wittinghofer\*

\* Max-Planck-Institut für molekulare Physiologie, Rheinlanddamm 201, 44139 Dortmund, Germany

† Max-Planck-Institut für medizinische Forschung, Jahnstr. 29, 69120 Heidelberg, Germany

**RAS-RELATED GTP-binding proteins function as molecular switches which cycle between GTP-bound 'on'- and GDP-bound 'off'-states<sup>1</sup>. GTP hydrolysis is the common timing mechanism that mediates the return from the 'on' to the 'off'-state. It is usually slow but can be accelerated by orders of magnitude upon interaction with GTPase-activating proteins (GAPs). In the case of Ras, a major regulator of cellular growth, point mutations are found in approximately 30% of human tumours which render the protein unable to hydrolyse GTP, even in the presence of Ras-GAPs. The first structure determination of a GTPase-activating protein reveals the catalytically active fragment of the Ras-specific p120GAP (ref. 2), GAP-334, as an elongated, exclusively helical protein which appears to represent a novel protein fold. The molecule consists of two domains, one of which contains all the residues conserved among different GAPs for Ras. From the location of conserved residues around a shallow groove in the central domain we can identify the site of interaction with Ras-GTP. This leads to a model for the interaction between Ras and GAP that satisfies numerous biochemical and genetic data on this important regulatory process.**

Five mammalian Ras-specific GAPs are known to date (summarized in ref. 3), in addition to several others from different organisms. Although of various sizes and domain composition they all contain the catalytic module, also called GAP-related domain, with characteristic blocks of sequence homology (Fig. 1a). p120GAP, the first GAP to be discovered<sup>2</sup>, is a protein of relative molecular mass 120,000 (*M<sub>r</sub>* 120K), consisting of several signalling domains<sup>4,5</sup> (Fig. 1b). Disruption of the gene in mice is embryonically lethal owing to vascular-system defects and neuronal apoptosis<sup>6</sup>. Neurofibromin (NF1), another Ras-GAP, is the product of the presumed tumour-suppressor gene *NFI* that is mutated or disrupted in patients suffering from type 1 neurofibromatosis<sup>7</sup>. Somatic mutations of the *NFI* gene are also found in solid tumours not associated with neurofibromatosis<sup>8</sup>. The importance of the proper functioning of the GTPase cycle is thus demonstrated by the occurrence of human diseases associated with mutations in either Ras itself or the regulatory proteins, both of which affect the rate of GTP hydrolysis and thus the regulation of cell growth. As a first step to investigate how GAPs might interact with Ras and stimulate Ras-mediated GTP hydrolysis, we have determined the crystal structure of GAP-334, a catalytically active fragment containing the 334 C-terminal residues of human p120GAP.

The structure of GAP-334 was determined with the multiple isomorphous replacement (MIR) method using mercury, gold and lead derivatives of crosslinked crystals<sup>9</sup> to solve the phase problem at 3 Å resolution. By using synchrotron radiation combined with cryocrystallography we obtained X-ray data of native crystals,

‡ Present address: Chester Beatty Laboratories, Fulham Road, London SW3 6JB, UK